TISSUE ENGINEERING: Part C
Volume 24, Number 7, 2018

DOI: 10.1089/ten.tec.2018.0024

termis
Tissue Engineering
& Regenerative Medicine
International Society

METHODS ARTICLE

In Vitro and *In Vivo* Correlation of Bone Morphogenetic Protein-2 Release Profiles from Complex Delivery Vehicles

Maurits G.L. Olthof, MD,[1–4] Marianna A. Tryfonidou, DVM, PhD,[4] Mahrokh Dadsetan, PhD,[1,2]
Wouter J.A. Dhert, MD, PhD,[4] Michael J. Yaszemski, MD, PhD,[1,2]
Diederik H.R. Kempen, MD, PhD,[5] and Lichun Lu, PhD[1,2]

Local sustained delivery of bioactive molecules from biomaterials is a promising strategy to enhance bone regeneration. To optimize delivery vehicles for bone formation, the design characteristics are tailored with consequential effect on bone morphogenetic protein-2 (BMP-2) release and bone regeneration. Complying with the 3R principles (Replacement, Reduction, and Refinement), the growth factor release is often investigated *in vitro* using several buffers to mimic the *in vivo* physiological environment. However, this remains an unmet need. Therefore, this study investigates the *in vitro-in vivo* correlation (IVIVC) of BMP-2 release from complex delivery vehicles in several commonly used *in vitro* buffers: cell culture model, phosphate buffered saline, and a strong desorption buffer. The results from this study showed that the release environment affected the BMP-2 release profiles, creating distinct relationships between release versus time and differences in extent of release. According to the guidance set by the U.S. Food and Drug Administration (FDA), IVIVC resulted in level A internal predictability for individual composites. Since the IVIVC was influenced by the BMP-2 loading method and composite surface chemistry, the external predictive value of the IVIVCs was limited. These results show that the IVIVCs can be used for predicting the release of an individual composite. However, the models cannot be used for predicting *in vivo* release for different composite formulations since they lack external predictability. Potential confounding effects of drug type, delivery vehicle formulations, and application site should be added to the equation to develop one single IVIVC applicable for complex delivery vehicles. Altogether, these results imply that more sophisticated *in vitro* systems should be used in bone regeneration to accurately discriminate and predict *in vivo* BMP-2 release from different complex delivery vehicles.

Keywords: bone morphogenetic protein-2 release, bone regeneration, *in vitro-in vivo* correlation, oligo(polyethelene glycol) fumarate

Introduction

Local sustained delivery of bioactive molecules from biomaterials is a promising strategy to enhance bone regeneration. Many studies have shown enhancement of bone formation in ectopic and orthotopic locations by sustained release of various growth factors.[1] Despite these promising results, improvement of the local delivery vehicles and optimization of the growth factor release profile remains a challenge.

New technologies have enhanced tailoring of release profiles within the challenging topic of designing the appropriate delivery vehicle for clinical application in bone regeneration. The biomaterials fulfill both a scaffold and delivery role, and need to meet various physical, mechanical, biological, and chemical demands. Tailoring the design characteristics may influence the growth factor release[2–5] with consequent differential effect on bone regeneration. As such, extensive *in vivo* animal studies are needed to analyze the release profiles and efficacy of the various delivery vehicles.

Departments of [1]Physiology and Biomedical Engineering and [2]Orthopedic Surgery, Mayo Clinic College of Medicine, Rochester, Minnesota.
[3]Department of Orthopaedics, University Medical Center Utrecht, Utrecht, The Netherlands.
[4]Department of Clinical Sciences of Companion Animals, Faculty of Veterinary Medicine, Utrecht University, Utrecht, The Netherlands.
[5]Department of Orthopaedic Surgery, Onze Lieve Vrouwe Gasthuis, Amsterdam, The Netherlands.

In contemporary scientific practice the 3R principles (Replacement, Reduction, and Refinement) are warranted. Therefore, to estimate the release kinetics, growth factor release is often investigated *in vitro* using several buffers to mimic the *in vivo* physiological environment.[6–8] Nonetheless, various studies have showed that *in vitro* release cannot be extrapolated to *in vivo* release.[9–11] To the best of our knowledge, there are no studies available that have attempted to correlate the *in vitro* and *in vivo* release profiles in the field of bone tissue engineering, and as such the relevance of these *in vitro* profiles for future clinical applications remains unknown. Therefore, the aim of this study is to investigate the *in vitro-in vivo* correlation (IVIVC) of growth factor release in several commonly used *in vitro* buffers and to develop a predictive model providing a standardized method employing a commonly used growth factor for these purposes.

IVIVC is defined by the U.S. Food and Drug Administration (FDA) as ''a predictive mathematical model describing the relationship between an *in vitro* property of a dosage form and relevant *in vivo* response.''[12] Several levels are described by the FDA protocol,[13] including level A up to D. Level A correlation represents a point-to-point relationship between *in vitro* and *in vivo* profiles. Level A correlation is considered most informative and is recommended by the FDA. It is the only level that can be used to obtain biowaiver. Level B correlation is based on the principles of statistical moment analysis but is devoid of a point-to-point correlation and hence does not reflect the actual *in vivo* release profile. As such, this level may lack sufficient predictability. Level C correlation establishes a single point relationship between dissolution and a pharmacokinetic parameter. Since it is based on a single point analysis, it is does not reflect the complete shape of the plasma concentration time curve, which is critical to define *in vivo* performance of the studied drug. Multiple Level C correlation relates multiple dissolution time points to one or more pharmacokinetic parameter(s) and should be based on at least three dissolution time points covering the early, middle, and late stages of the dissolution profile. A multiple Level C correlation can be as useful as a Level A correlation. However, if a multiple Level C correlation is achieved, the development of a Level A correlation is feasible and preferred. Level D correlation is a rank order correlation comparing *in vitro* and *in vivo* release profiles. A level D correlation is only qualitative and is not adopted in the FDA IVIVC Guidance.

Given that level A IVIVC is the most informative, this study employs this correlation level to accurately predict the *in vivo* performance from the *in vitro* performance. Bone morphogenetic protein-2 (BMP-2), a promising bone formation inducing agent, was used and released from several biomaterial composites to investigate the internal and external predictability of the IVIVC. The IVIVC for locally delivered drugs, such as BMP-2, is challenging due to complex characteristics of the biomaterials and lack of a standardized *in vitro* model. Therefore, level A IVIVC was analyzed for composites with various characteristics releasing BMP-2 in several *in vitro* models as a first step toward determining the proper *in vitro* system and developing a predictive model for *in vivo* release of BMP-2. Furthermore, to make a qualitative assessment of the IVIVC, a rank order level D IVIVC between the different composites was performed.

Materials and Methods

Experimental design

To investigate the relationship between *in vitro* and *in vivo* BMP-2 release kinetics, various composites with predicted differential release profiles were studied in three *in vitro* models. The composites were based on 75% porous oligo(polyethelene glycol) fumarate (OPF) hydrogels (22.5% w/w) containing 2.5% (w/w) poly(lactic-co-glycolic acid) (PLGA) microspheres. The BMP-2 loading method and hydrogel chemical properties were modified to achieve distinct BMP-2 release kinetics. These results were described in previous articles.[14,15] BMP-2 was encapsulated in PLGA microspheres and/or adsorbed on the hydrogel to create hydrogels with different burst and sustained release of BMP-2. Apart from the different loading methods, hydrogel chemistry was modified to further tailor BMP-2 release by cross-linking sodium methacrylate (SMA; Sigma-Aldrich, St. Louis, MO), [2-(methacryloyloxy) ethyl]-trimethylammonium chloride (MAE; Sigma-Aldrich) or bis[2-(methacryloyloxy)ethyl] (BP) into the hydrogel to obtain negatively charged OPF (n-OPF), positively charged OPF (p-OPF) and phosphate modified hydrogels OPF (Ph-OPF), respectively. These modifications resulted in a total of 12 different composites (Table 1).

The *in vitro* and *in vivo* BMP-2 release was evaluated by employing BMP-2 radiolabeled with ^{125}I. To simulate the cell-rich *in vivo* environment, *in vitro* release of all composites was investigated using a cell culture setup for 8 weeks. To analyze the influence of different commonly used *in vitro* buffers on *in vitro* BMP-2 release, a subset of composites was immerged in a cell-free environment in the presence of phosphate buffered saline (PBS) or a strong desorption buffer (SDB). The *in vivo* BMP-2 release was analyzed in a subcutaneous rat model with 8 weeks' follow-up. Subsequently, the IVIVC level A was investigated for all *in vitro* release systems.

BMP-2 radioiodination

Carrier-free Na^{125}I was obtained from PerkinElmer Life and Analytical Sciences (Boston, MA). To study the release profiles of BMP-2, a fraction of the incorporated BMP-2 was radiolabeled with ^{125}I, using the chloramine-T method as previously described.[16] The radiolabeled BMP-2 was separated from the free ^{125}I by 24-h dialysis (10 kDa molecular weight cutoff [MWCO]; SpectraPor 7, Rancho Dominguez, CA) against 0.01 M phosphate buffered saline at pH 7.4 (Sigma-Aldrich). The ^{125}I-BMP-2 dialysate was concentrated in a Millipore device (10 kDa MWCO, Billerica, MA) and the purity was determined by trichloroacetic acid precipitation. The final ^{125}I-BMP-2 preparation contained 99.7% precipitable counts, which indicated the percentage of covalently bound ^{125}I to the BMP-2. Thereafter, ^{125}I-BMP-2 was mixed with nonlabeled BMP-2 (1:5.3 hot–cold ratio) and incorporated into the composite formulations.

Microsphere fabrication

PLGA 50:50 (M_w 52 kDa; Lakeshore Biomaterials) microspheres were fabricated using a double-emulsion-solvent-extraction (W1-O-W2) technique according to a previously described method.[17] Briefly, an aqueous solution containing 130 μL (OPF-Msp), 65 μL (OPF-Cmb), or 0 μL

Table 1. Summary of Composite Characteristics Used in the *In Vitro* and *In Vivo* Bone Morphogenetic Protein-2 Release Studies

Composite name	*BMP-2 loading*		*Initial activity/ implant (μCi)*	*BMP-2/ implant (μg)*	In vitro *buffer*
	Hydrogel	*Microspheres*			
-OPF-Msp	0% Adsorbed	100% Loaded	3.7 ± 0.8	4.7 ± 1.0	CC
-OPF-Cmb	50% Adsorbed	50% Loaded	3.5 ± 0.2	4.6 ± 0.2	CC, PBS, SDB
-OPF-Ads	100% Adsorbed	0% Loaded	3.8 ± 0.2	4.9 ± 0.3	CC, PBS, SDB
n-OPF-Msp	0% Adsorbed	100% Loaded	3.0 ± 0.5	3.8 ± 0.6	CC
n-OPF-Cmb	50% Adsorbed	50% Loaded	2.7 ± 0.2	3.6 ± 0.2	CC, PBS, SDB
n-OPF-Ads	100% Adsorbed	0% Loaded	3.0 ± 0.1	4.0 ± 0.1	CC, PBS, SDB
p-OPF-Msp	0% Adsorbed	100% Loaded	2.4 ± 0.3	3.1 ± 0.4	CC
p-OPF-Cmb	50% Adsorbed	50% Loaded	2.3 ± 0.1	3.0 ± 0.2	CC, PBS, SDB
p-OPF-Ads	100% Adsorbed	0% Loaded	2.5 ± 0.1	3.2 ± 0.2	CC, PBS, SDB
Ph-OPF-Msp	0% Adsorbed	100% Loaded	3.1 ± 0.1	4.0 ± 0.1	CC
Ph-OPF-Cmb	50% Adsorbed	50% Loaded	3.0 ± 0.2	3.9 ± 0.3	CC
Ph-OPF-Ads	100% Adsorbed	0% Loaded	3.1 ± 0.6	4.0 ± 0.7	CC

Ads, adsorbed BMP-2; BMP-2, bone morphogenetic protein-2; CC, *in vitro* cell culture model; Cmb, combined microsphere encapsulated and adsorbed BMP-2; Msp, microsphere encapsulated BMP-2; n-OPF, negatively charged OPF; OPF, oligo(polyethelene glycol) fumarate; -OPF, unmodified OPF; PBS, phosphate buffered saline; Ph-OPF, phosphate modified OPF; p-OPF, positively charged OPF; SDB, strong desorption buffer.

(OPF-Ads) of 3.7 mg/mL ^{125}I-BMP-2/BMP-2 (1:5.3 hot:cold ratio) solution was emulsified with 250 mg PLGA 50:50 dissolved in 1.25 mL of dichloromethane using a vortex at 3050 rpm. The solution was re-emulsified in 2 mL of 2% (w/v) aqueous poly(vinyl alcohol) (PVA, 87–89% mole hydrolyzed, M_w = 13,000–23,000; Sigma-Aldrich) to create the double emulsion and added to 100 mL of a 0.3% (w/v) PVA solution and 100 mL of a 2% (w/v) aqueous isopropanol solution. After 1 h of slow stirring, the PLGA microspheres were collected by centrifugation at 2500 rpm for 3 min, washed three times with distilled deionized water (ddH_2O), and freeze dried to a free-flowing powder. The characteristics of the PLGA microspheres were reported in a previous study.[14] The diameter of both unloaded and BMP-2-loaded microspheres was distributed between 0 and 100 μm. The PLGA microspheres used in this study lose ~80% of their mass within 4 weeks after implantation.[18]

Fabrication of composites

OPF was fabricated using polyethylene glycol (PEG) with an initial molecular weight of 10 kDa according to previously described method.[19] OPF (44% w/w), N-vinyl pyrrolidinone (13% w/w [NVP]; Sigma-Aldrich), Irgacure 2959 (0.2%; Ciba-Specialty Chemicals, Tarrytown, NY), and H_2O (42% w/w) were mixed with either SMA (200 mg, 8.2% w/w; Sigma-Aldrich), MAE (225 mg, 10.3% w/w; Sigma-Aldrich), or no additive to create hydrogels with a fixed negative (n-OPF), positive (p-OPF), or neutral (-OPF) charge, respectively. For Ph-OPF, OPF (41% w/w), NVP (29% w/w; Sigma-Aldrich), BP (8.2% w/w), and Irgacure 2959 (0.2% w/w; Ciba-Specialty Chemicals) were dissolved in deionized water (21.6% w/w).

To create the composites, the OPF/NVP, OPF/NVP/SMA, OPF/NVP/MAETAC, or OPF/NVP/BP paste (22.5% w/w) was mixed with NaCl salt particles (75% w/w, sieved to a maximal size of 300 μm) and PLGA microspheres (2.5% w/w). The resulting mixture was forced into a cylindrical mold with a diameter of 3.5 mm and exposed to ultraviolet light (365 nm at intensity of ~8 mW/cm^2 black-Ray Model 100AP, Upland, CA) to cross-link the composites for 40 min in total. The composite implants were cut into 6 mm long rods, sterilized by ethanol evaporation for both the *in vitro* and *in vivo* experiments, and immersed in sterile ddH_2O to leach out the salt. After blot drying, additional BMP-2 was loaded on the composite matrix by adsorption for the OPF-Cmb and OPF-Ads scaffolds. By varying the BMP-2 loading method, three different composite implants were created consisting of 100% of the BMP-2 encapsulated in PLGA microspheres (OPF-Msp, sustained release), 50% of the BMP-2 encapsulated in PLGA microspheres, and 50% adsorbed on the composite (OPF-Cmb, combined burst and sustained release), and 100% adsorbed on the composite (OPF-Ads, mainly burst release) (Table 1).

The bioactivity of the released BMP-2 was reported previously and showed a similar bioactivity for the microsphere encapsulated and adsorbed growth factor after 9 weeks of release.[14] Also, the released BMP-2 generated a similar biologic response compared to freshly added BMP-2 of corresponding dose *in vitro*. The degradation rate of the OPF hydrogel is reported previously and was slow with minimal *in vitro* degradation of cross-linked hydrogels with an OPF:NVP ratio >0.3 after 21 days in PBS.[20] Furthermore, histology shows a still visible porous structure of OPF after 9 weeks of implantation, as opposed to a fully resorbed Infuse® absorbable collagen sponge (Medtronic, Minneapolis, MN).[14]

In vivo *release measurements*

Thirty-two 12-week-old male Harlan Sprague Dawley rats were used for this study according to an approved protocol by the local animal care and use committee. Animal studies were previously published.[14,15] Surgery was performed under sterile conditions and general anesthesia (ketamine/xylazine, 45/10 mg/kg). After shaving and disinfecting the surgical sites, subcutaneous pockets were created in each limb and filled with ^{125}I-BMP-2-loaded implants.

Two subcutaneous pockets in the thoracolumbar region were used to implant the controls (unloaded implants). Acetaminophen (160 mg in 5 mL added to pint water bottle) was given as postoperative analgesia for the duration of 1 week. Four scintillation probes (model 44–3 low energy gamma scintillator; Ludlum Measurements, Inc.) connected to digital scalers (Model 1000 scaler; Ludlum Measurements, Inc.) as described previously,[17] were used for determining *in vivo* ^{125}I-BMP-2 release kinetics. Directly after wound closure, the ^{125}I-BMP-2 activity was measured to determine the starting implanted dose. At each subsequent time point (biweekly the first week, weekly from week 1 onward), the rats were anesthetized using isoflurane (induction 4%, maintenance >1.5%) to measure the local ^{125}I-BMP-2 activity in duplicate over two 1-min periods. To determine the BMP-2 release, the ^{125}I-BMP-2 measurements were corrected for radioactive decay and background activity. The ^{125}I-BMP-2 activity was normalized to the starting implanted dose to determine the retained ^{125}I-BMP-2 dose and released amounts. After 9 weeks, the rats were euthanized by CO_2 asphyxiation.

In vitro *BMP-2 release*

BMP-2 release was analyzed using a W20-17 cell culture system. The composites were exposed to consecutive 7-day cell cultures (seeded at 20,000 cells per cm^2 in a 24-well plate) in 1 mL Dulbecco's Modified Eagle's Medium/Nutrient Mixture F-12 Ham 1:1 mixture (DMEM/F12; Sigma-Aldrich) supplemented with 10% fetal bovine serum and 1% penicillin at 37°C, 20% O_2, 5% CO_2. A subset of composites was analyzed for BMP-2 release in the presence of PBS (pH 7.4) or SDB (solution containing 0.5 M arginine, 0.5 M NaCl and 50 mM K_2HPO_4 in ddH_2O at pH of 7.5). The composites were placed in 1.0 mL PBS or SDB containing Eppendorf tubes and maintained at 37°C in the incubator. At weeks 0.5, 1, 2, 3, 4, 5, 6, 7, and 8, the culture medium was collected and replaced with fresh DMEM/F12, PBS or SDB. To determine the BMP-2 release, the collected culture medium was assayed for ^{125}I activity on a gamma counter. At the end of the study, the composites were collected to determine the remaining ^{125}I activity as a measure of retained BMP-2. All ^{125}I activity measurements were corrected for decay and normalized to the starting amount. The corresponding *in vitro* release profiles were determined by correlating the gamma-irradiation in counts/minute to the amount of BMP-2 released from the composites.

In vitro-in vivo *correlation*

The data acquired in the release studies were used to develop the IVIVC. The IVIVC was obtained by correlating the composites cumulative release *in vitro* with the cumulative *in vivo* release. Regression analysis was applied to the IVIVC plots and the corresponding equations described. To analyze the external predictive value of the *in vitro* models, superimposability of the IVIVCs was tested for composites with similarly expected release mechanisms. Therefore, OPF-Msp composites (expected to release BMP-2 mainly by polymer degradation and diffusion), OPF-Cmb composites (expected to release BMP-2 mainly by polymer degradation, diffusion, desorption, and ion exchange), and OPF-Ads composites (expected to release BMP-2 mainly by desorption and ion exchange) were analyzed for external predictability separately. To accurately predict the *in vivo* BMP-2 release profile, a point-to-point IVIVC is needed. Therefore, levels B and C were considered not suitable for developing a clinically relevant predictive model. To make a qualitative assessment of the IVIVCs, level D IVIVC was analyzed using the cumulative BMP-2 release of the different composites in the various release environments.

Statistical analysis

Statistical analysis was performed using Prism 7 (Graphpad Software, La Jolla, CA) and SPSS 22.0 software (SPSS, Inc., Chicago, IL). *In vitro* results ($n=3$ per composite type studied) and *in vivo* results ($n=10$ for -OPF, n-OPF, p-OPF, and Ph-OPF-Cmb; and $n=8$ for Ph-OPF-Msp and Ph-OPF-Ads) of BMP-2 release are given as mean ± standard deviation. The BMP-2 release was analyzed point-to-point for a period of 8 weeks *in vitro* and *in vivo*. All datasets were tested for outliers using Hoaglin's outlier labeling rule,[21] for normality of the residuals using the Shapiro-Wilk test and for homogeneity of variances using the Levene's test. Parametric data were analyzed with univariate analysis of variances and Benjamini Hochberg *post hoc*. Radar diagrams were used to illustrate the extent of cumulative BMP-2 release and ranking of the different composites in the various release environments (*in vitro* and *in vivo*). To analyze the predictive value of *in vitro* release for *in vivo* BMP-2 release different regression models were analyzed for fit using R^2.

Results

BMP-2 labeling and incorporation

Labeling of the BMP-2 with ^{125}I resulted in an activity per mass of 6.1 μCi/μg. The microspheres were loaded with either 2.9 μg BMP-2/mg PLGA (OPF-Msp) or 1.3 μg BMP-2/mg PLGA (OPF-Cmb). The composite scaffold characteristics are summarized in Table 1. The different loading methods resulted in comparable BMP-2 loading per scaffold. OPF modifications aiming at composite chemistry resulted in differences in BMP-2 loading (<1.9 μg BMP-2) within chemistry modifications due to differences in BMP-2 loss during the fabrication process (Table 1). To correct for this, the release kinetics were corrected for the starting amount of BMP-2 loading for each individual composite both *in vitro* and *in vivo*.

Animals

Five rats died 1 day after surgery, probably due to oversensitivity to xylazine, since no health problems were observed in the remainder of the rats after the xylazine was lowered. Nine implants were removed by the rats themselves from the subcutaneous pocket during the follow-up and were therefore discarded from further analysis. Detailed information on sample size used for each analysis is provided in Supplementary Table S1 (Supplementary Data are available online at www.liebertpub.com/tec).

In vivo *and* in vitro *release profiles*

As expected, the composites showed different *in vivo* BMP-2 release profiles. Most composites demonstrated a triphasic *in vivo* release profile with a large burst release phase (Phase 1, till week 0.5), high dose sustained release phase (Phase 2, weeks 0.5–5) and a low dose zero order release phase (Phase 3, week 5 onward) (Fig. 1A). After the large burst release, various release patterns were seen for the different OPF-composites in phase 2, including exponential growth, exponential decay and linear relationships of BMP-2 release versus time (Fig. 2). In Phase 3 all composites showed a linear relationship with different BMP-2 release rates. Ph-OPF-Msp and Ph-OPF-Cmb exhibited a tetraphasic *in vivo* release profile, with the high sustained release phase 2 divided into a lag phase and rapid release phase (Fig. 2).

Although different release profiles were observed *in vitro* compared to *in vivo*, the triphasic time frames were similar. In the cell culture set-up, the composites exhibited different burst releases in phase 1, exponential decay release profiles with large variability in phase 2, and zero order release in phase 3 (Fig. 1B). In PBS, a minimal burst release was observed for all composites, a near linear exponential decay release profile in phase 2, and a zero-order release in phase 3 (Fig. 1C). Minimal differences were observed between the composites in SDB. After the burst release with minimal variability, similar exponential decay patterns were seen for all composites during phases 2 and 3 (Fig. 1D). Since every phase showed different relationships for BMP-2 release versus time, the phases were analyzed for IVIVC level A separately. Phases 1 and 2 were considered most relevant since *in vivo* most composites released >80% BMP-2 till week 5 and low dose release was observed from week 5 onward for all composites.

In vitro-in vivo *correlations*

Level A IVIVC

All phases. For the cell culture model, OPF-Msp composites showed linear regression relationship ($R^2 > 0.90$) with residuals <19.6% (Fig. 3A). Similarly, OPF-Cmb composites showed linear regression relationships ($R^2 > 0.91$) with residuals <14.2% between *in vitro* and *in vivo* in the cell culture model (Fig. 3B). The OPF-Ads composites showed exponential decay regression relationships ($R^2 > 0.99$) with residuals <3.0% (Fig. 3C). For the cell-free PBS buffer, OPF-Cmb composites showed linear regression relationships ($R^2 > 0.95$) with residuals <9.4% (Fig. 3D). OPF-Ads composites showed an exponential decay relationship ($R^2 > 0.99$) with residuals <1.0% between *in vitro* and *in vivo* (Fig. 3E). For the cell-free SDB buffer, OPF-Cmb composites showed linear and exponential

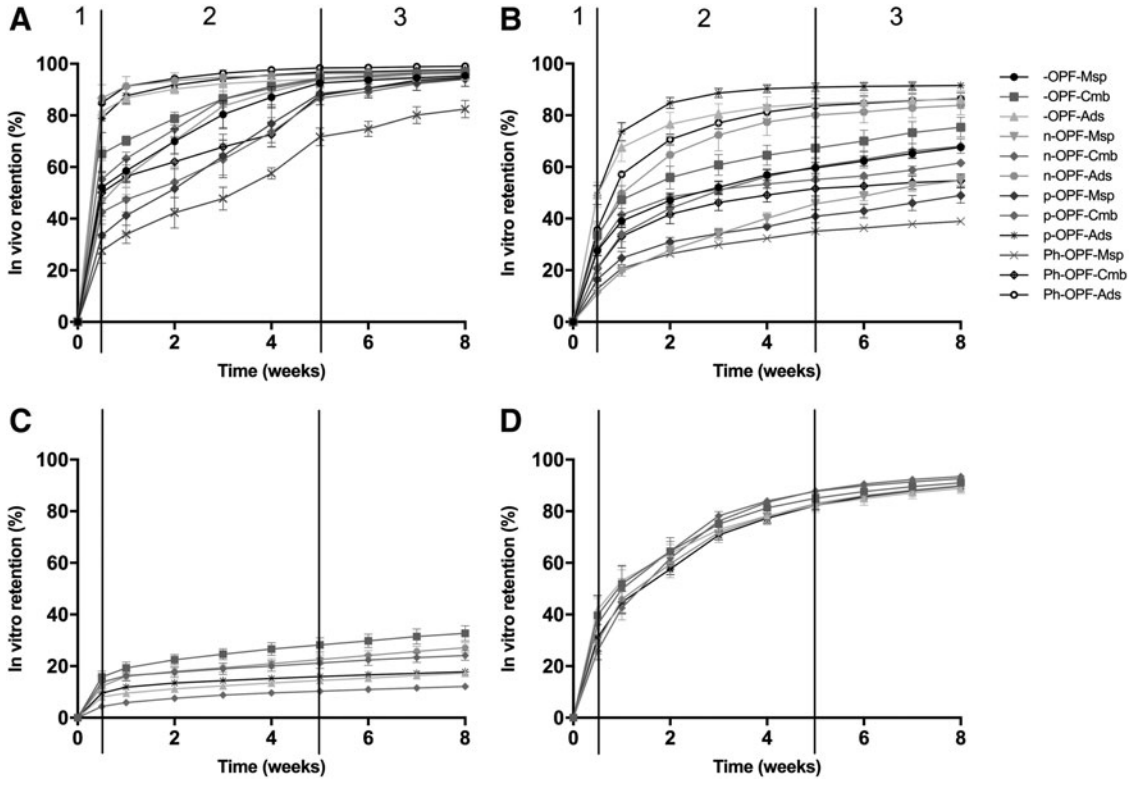

FIG. 1. Cumulative release of BMP-2 from various polymer composites *in vivo* in a rat subcutaneous implantation model **(A)** or [CC **(B)**, PBS **(C)**, SDB **(D)**]. The release profiles are divided into three phases, burst release (phase 1), high dose release sustained release (phase 2), and low dose sustained release (phase 3). Ads, adsorbed BMP-2; BMP-2, bone morphogenetic protein-2; CC, in vitro cell culture model; Cmb, combined microsphere encapsulated and adsorbed BMP-2; Msp, microsphere encapsulated BMP-2; n-OPF, negatively charged OPF; OPF, oligo(polyethelene glycol) fumarate; -OPF, unmodified OPF; PBS, *in vitro* phosphate buffered saline; Ph-OPF, phosphate modified OPF; p-OPF, positively charged OPF; SDB, *in vitro* strong desorption buffer model.

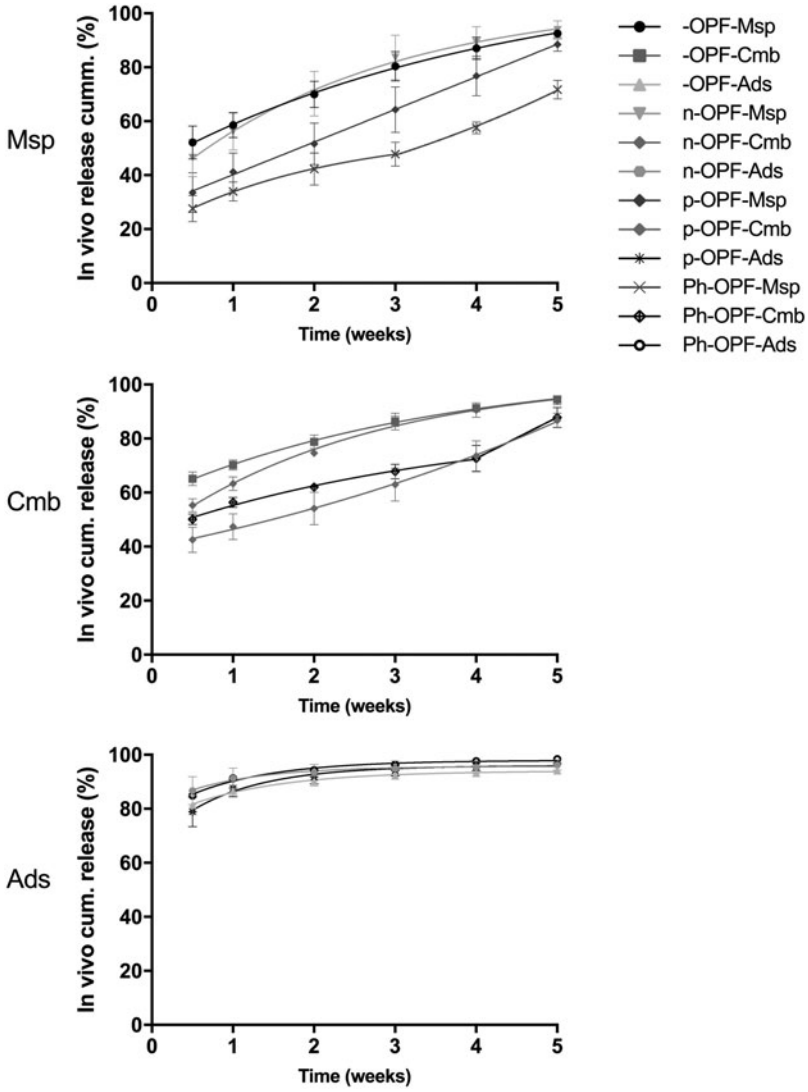

FIG. 2. Relationship between the cumulative release of BMP-2 (%) *in vivo* in a rat subcutaneous model and time for the low dose sustained release phase (phase 2). Various release patterns were observed for the different OPF-composites in phase 2, including exponential growth, exponential decay, and linear relationships of BMP-2 release versus time.

regression relationships ($R^2 > 0.99$) with residuals <13.1% (Fig. 3F). The OPF-Ads composites showed an exponential decay relationship ($R^2 > 0.99$) with residuals <1.8% between *in vitro* and *in vivo* (Fig. 3G).

The confounding effect of the surface chemistry of the composites on the relationship, slope, span, and *X*- and *Y*-intercepts of the IVIVCs, influenced the regression models of all IVIVCs (Fig. 3). The acquired models were not superimposable and therefore lacked external predictability. Since a large area had to be extrapolated for the large burst release phase, the burst release phase and sustained release phase were analyzed for IVIVC separately.

Phase 1 (burst release phase). In the cell culture setup, the burst release from the different composites showed a strong linear correlation ($R^2 = 0.68$) with the *in vivo* burst release and residuals <11% released BMP-2 (Fig. 4A, B). In the subset of composites the correlation between *in vitro* and *in vivo* BMP-2 burst release was very weak in PBS ($R^2 = 0.06$) and SDB ($R^2 = 0.07$), and moderate in the cell culture setup ($R^2 = 0.45$) (Fig. 4C, D).

Phases 2 and 3 (sustained release phase). For the cell culture model (Table 2), the OPF-Msp composites showed a sigmoidal regression relationship ($R^2 > 0.99$) with residuals <2.2% (Fig. 5A). Similarly, the OPF-Cmb composites showed sigmoidal regression relationship ($R^2 > 0.98$) with residuals <4% (Fig. 5B). A linear regression relationship ($R^2 > 0.97$) was observed for OPF-Ads composites with residuals <1.8% (Fig. 5C). For the cell-free PBS *in vitro* model (Table 3), OPF-Cmb composites showed sigmoidal regression relationship ($R^2 > 0.99$) with residuals <3.1% (Fig. 5D). OPF-Ads composites showed exponential decay regression relationships ($R^2 > 0.99$) with residuals <0.6% (Fig. 5E). For the cell-free SDB *in vitro* model (Table 3), OPF-Cmb composites showed sigmoidal ($R^2 > 0.99$, -OPF, n-OPF) and exponential growth ($R^2 > 0.94$, p-OPF) regression relationships with <0.7% (-OPF, n-OPF) and <8.7% released BMP-2 (p-OPF) residuals (Fig. 5F). OPF-Ads composites showed an exponential decay relationship ($R^2 > 0.99$) with residuals <0.6% (Fig. 5G).

The confounding effect of the surface chemistry of the composites on the relationship, slope, span, and *X*- and *Y*-intercepts of the IVIVCs, influenced the regression models

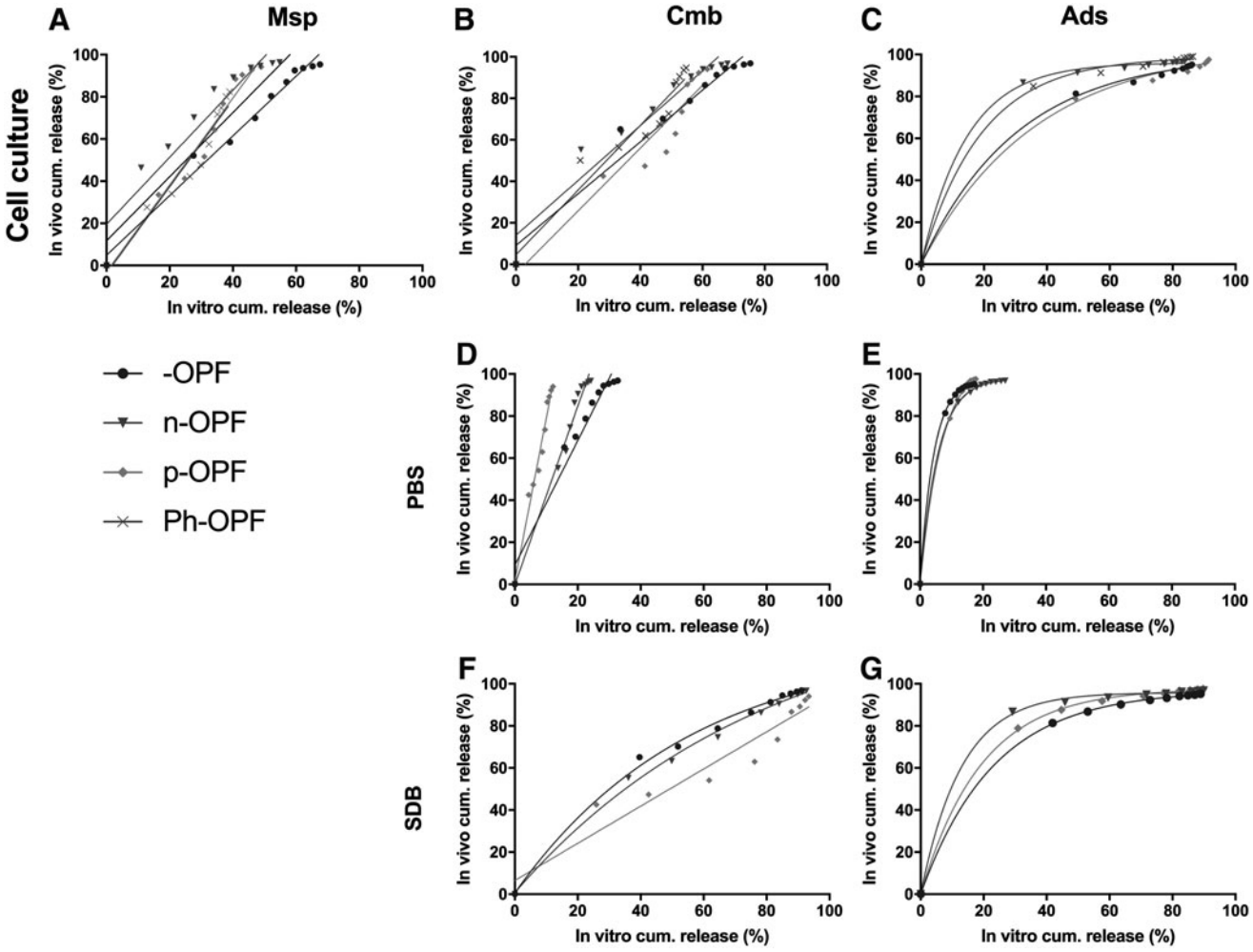

FIG. 3. Level A *in vitro* (CC, PBS, and SDB)-*in vivo* correlations (IVIVCs) of cumulative BMP-2 release (%) for the different OPF composites for all time points. The figure is horizontally divided into different *in vitro* models and vertically divided into different BMP-2 loading methods.

of all IVIVCs (Fig. 5). The acquired models were not superimposable and therefore lacked external predictability.

Level D IVIVC. Level D IVIVC of BMP-2 release in the various conditions is shown per time-point in radar diagrams (Fig. 6) to analyze the rank order and extent of release of the different composites in the various release environments. The burst release varied in extent of release and ranking for the different composites. The variation in burst release between the different composites was minimal in the cell-free PBS and SDB, whereas large differences were observed between the composites in the cell culture model and *in vivo*. Furthermore, the ranking of the implants differed per release environment. For example, n-OPF-Ads had the highest burst release *in vivo*, but ranked fourth in cell culture set up, third in PBS, and fifth in SDB. Differences in ranking and extent of cumulative BMP-2 release were also observed for the different release environments in the sustained release phase up to 8 weeks.

Discussion

The BMP-2 release profiles and IVIVC of various complex composites were investigated in several *in vitro* release environments. The latter affected the BMP-2 release profiles, creating distinct different relationships between release versus time and differences in extend of release. IVIVC resulted in level A internal predictability for individual composites. However, since the IVIVC was influenced by the BMP-2 loading method and composite surface chemistry, the external predictive value of *in vivo* release based on the *in vitro* and *in vivo* relationship was limited, stressing thereby the importance of including these cofounders in future IVIVC models.

The release environments influenced the BMP-2 release profiles differently. A large variation was seen in release profiles between the different composites *in vivo* and in the cell culture, whereas limited differences were seen in the cell-free *in vitro* environments. Although variation in cumulative release was observed in the cell culture model, the rank orders of the composites were different compared to *in vivo*. Despite the limited differences, the rank order also differed between PBS or SDB and *in vivo*. Furthermore, the *in vivo* relationship between release and time was not accurately predicted by the *in vitro* models. These results indicate that these *in vitro* models are not able to mimic the complex *in vivo* drug release conditions. Certain *in vivo*

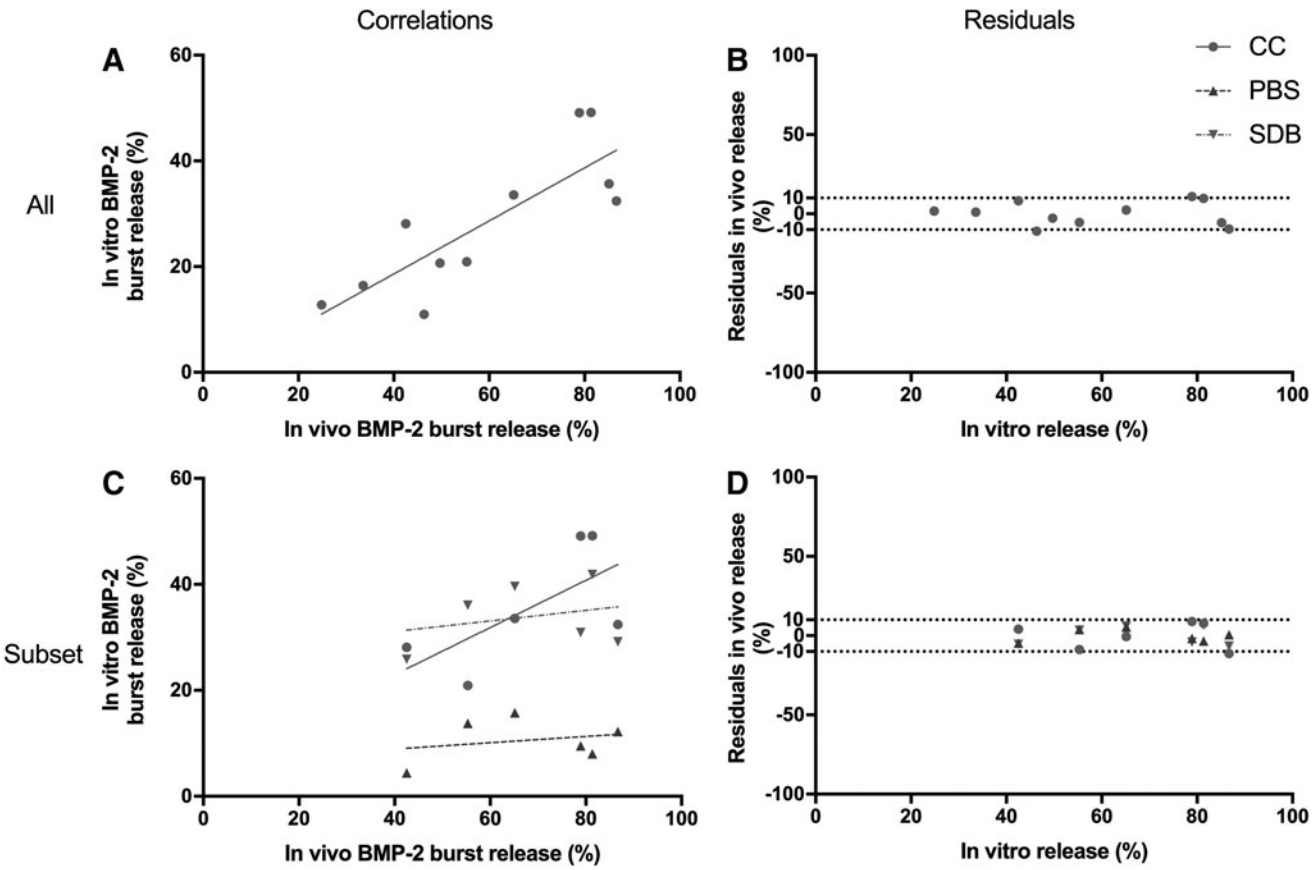

FIG. 4. Level A *in vitro* (CC, PBS, and SDB)-*in vivo* correlations (IVIVCs) of the BMP-2 burst release phase 1 for the all OPF composites **(A, B)** and a subset of composites (OPF-Cmb/Ads, n-OPF-Cmb/Ads, and p-OPF-Cmb/Ads) **(C, D)** with corresponding residuals.

environmental differences could have explained differences in polymer erosion, drug diffusion, ion exchange, and desorption with subsequent differences in release profiles. For example, in PLGA foams, *in vivo* degradation was accelerated by an autocatalytic effect of the degradation products of the polymer.[22] Furthermore, resident cells, proteins and ions could have influenced the polymer erosion, ion exchange, and desorption *in vivo*.[23–26] The superior *in vivo* reflection of the cell culture model against the cell-free *in vitro* models highlights the profound effect of biological influences on release profiles.

The various release phases affected the IVIVCs from the different composites. Since the *in vivo* burst release of the composites was >25% and no data points were available within this period, a large interval of the IVIVCs had to be extrapolated questioning the validity of the findings regarding

Table 2. Internal Predictive *In Vitro-In Vivo* Correlation Level A Characteristics for the Sustained Release Phase in a Cell Culture Model

Composite name	*Relationship*	R^2	*Model*
-OPF-Msp	Sigmoidal	0.998	$Y = 51 + (98-51)/(1+10\text{^}[\{49 - X\} \times 0.08])$
-OPF-Cmb	Sigmoidal	0.998	$Y = 65 + (98-65)/(1+10\text{^}[\{58 - X\} \times 0.08])$
-OPF-Ads	Linear	0.986	$Y = 0.38 \times X + 62.25$
n-OPF-Msp	Sigmoidal	0.999	$Y = 41 + (97-41)/(1+10\text{^}[\{27 - X\} \times 0.06])$
n-OPF-Cmb	Sigmoidal	0.999	$Y = 54 + (99-54)/(1+10\text{^}[\{44 - X\} \times 0.06])$
n-OPF-Ads	Linear	0.989	$Y = 0.19 \times X + 81.17$
p-OPF-Msp	Sigmoidal	0.997	$Y = 35 + (95-35)/(1+10\text{^}[\{34 - X\} \times 0.1])$
p-OPF-Cmb	Sigmoidal	0.991	$Y = 45 + (96-45)/(1+10\text{^}[\{53 - X\} \times 0.2])$
p-OPF-Ads	Linear	0.971	$Y = 0.43 \times X + 56.85$
Ph-OPF-Msp	Sigmoidal	0.995	$Y = 28 + (107-28)/(1+10\text{^}[\{35 - X\} \times 0.09])$
Ph-OPF-Cmb	Sigmoidal	0.981	$Y = 52 + (160-52)/(1+10\text{^}[\{57 - X\} \times 0.07])$
Ph-OPF-Ads	Linear	0.998	$Y = 0.28 \times X + 75.15$

Models were based on a sigmoidal function $Y = \text{bottom} + (\text{top} - \text{bottom})/(1+10\text{^}[\{\log EC50 - X\} \times \text{hillslope}])$ and a linear function $Y = \text{slope} \times X + Y\text{-intercept}$.

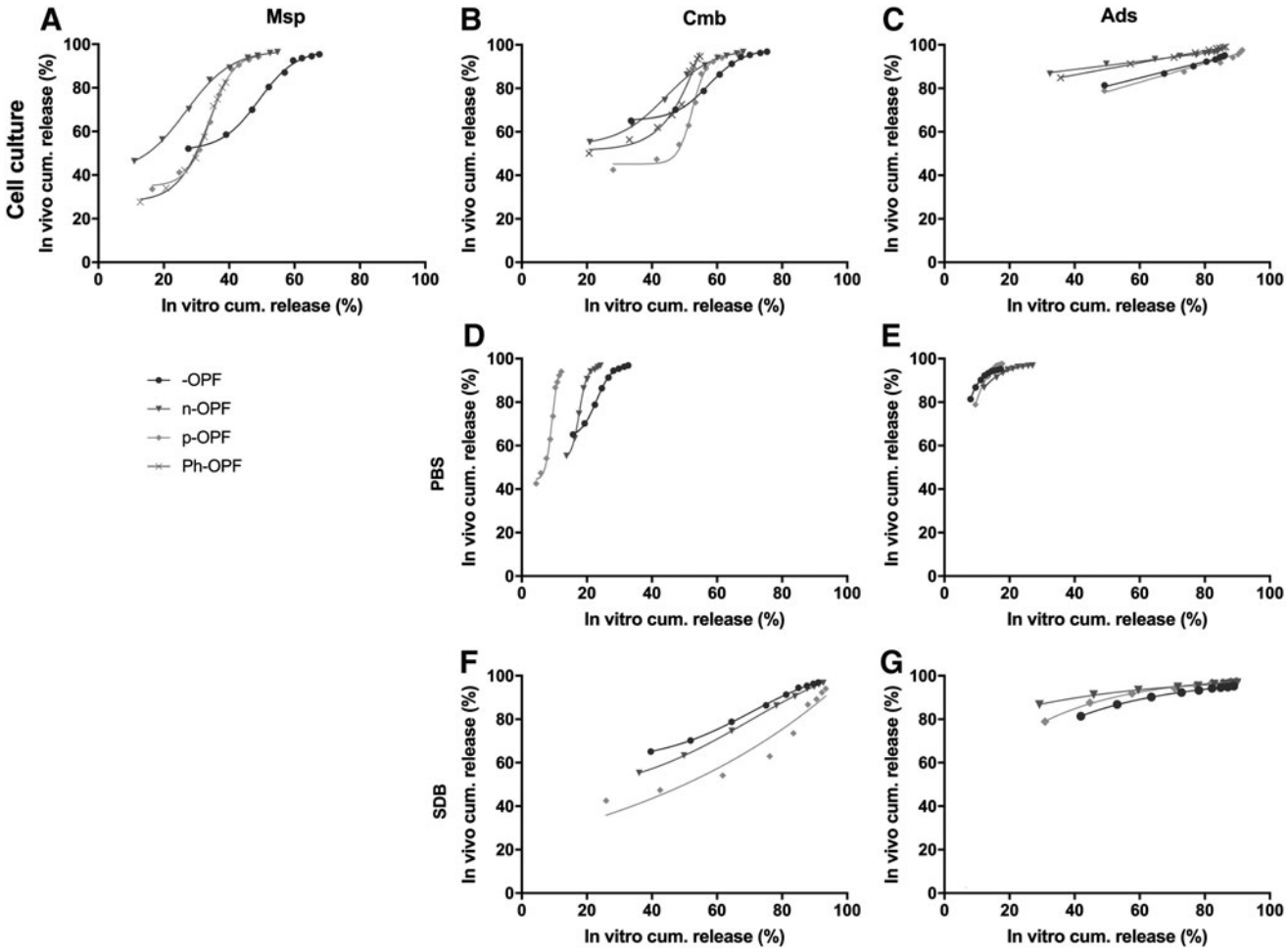

FIG. 5. Level A *in vitro* (CC, PBS, and SDB)-*in vivo* correlations (IVIVCs) of cumulative BMP-2 release (%) for the different OPF composites for the sustained release phase (phase 2, 3). The figure is horizontally divided into different *in vitro* models and vertically divided into different BMP-2 loading methods.

this phase of release. Therefore, the burst and sustained release phase of the different composites was also analyzed separately. IVIVCs beyond the burst release phase showed models with better fit and internal predictability compared to all phases combined. In line with this, high burst releases are associated with lower correlating IVIVCs.[27] Rapid burst release phase from microencapsulated drugs may be related to the onset of bulk erosion of the polymer, providing additional pores for diffusion of the entrapped protein.[28] Since the rate limiting step of drug availability is drug permeability across

TABLE 3. INTERNAL PREDICTIVE *IN VITRO-IN VIVO* CORRELATION LEVEL A CHARACTERISTICS FOR THE SUSTAINED RELEASE PHASE IN CELL-FREE *IN VITRO* BUFFERS

Release buffer	*Composite name*	*Relationship*	R^2	*Model*
PBS	-OPF-Cmb	Sigmoidal	0.999	$Y = 64 + (97 - 64)/(1 + 10\text{^}[\{23 - X\} \times 0.2])$
	-OPF-Ads	Exponential decay	0.999	$Y = (-64 - 96) \times \exp(-0.3 \times X) + 96$
	n-OPF-Cmb	Sigmoidal	0.999	$Y = 54 + (96 - 54)/(1 + 10\text{^}[\{18 - X\} \times 0.4])$
	n-OPF-Ads	Exponential decay	0.992	$Y = (17 - 98) \times \exp(-0.2 \times X) + 98$
	p-OPF-Cmb	Sigmoidal	0.992	$Y = 44 + (98 - 44)/(1 + 10\text{^}[\{9 - X\} \times 0.4])$
	p-OPF-Ads	Exponential decay	0.996	$Y = (-88 - 102) \times \exp(-0.2 \times X) + 102$
SDB	-OPF-Cmb	Sigmoidal	0.999	$Y = 60 + (106 - 60)/(1 + 10\text{^}[\{70 - X\} \times 0.03])$
	-OPF-Ads	Exponential decay	0.999	$Y = (33 - 99) \times \exp(-0.03 \times X) + 99$
	n-OPF-Cmb	Sigmoidal	0.999	$Y = 44 + (114 - 44)/(1 + 10\text{^}[\{70 - X\} \times 0.02])$
	n-OPF-Ads	Exponential decay	0.998	$Y = (74 - 100) \times \exp(-0.02 \times X) + 100$
	p-OPF-Cmb	Exponential growth	0.937	$Y = 25 \times \exp(0.01 \times X)$
	p-OPF-Ads	Exponential decay	0.997	$Y = (38 - 100) \times \exp(-0.04 \times X) + 100$

Models were based on a sigmoidal function $Y = \text{bottom} + (\text{top} - \text{bottom})/(1 + 10\text{^}[\{\text{logEC50} - X\} \times \text{hillslope}])$, an exponential decay function $Y = (Y0 - \text{plateau}) \times \exp(-\text{K} \times X) + \text{plateau}$, an exponential growth function $Y = Y0 \times \exp(\text{K} \times X)$, and a linear function $Y = \text{slope} \times X + Y\text{-intercept}$.

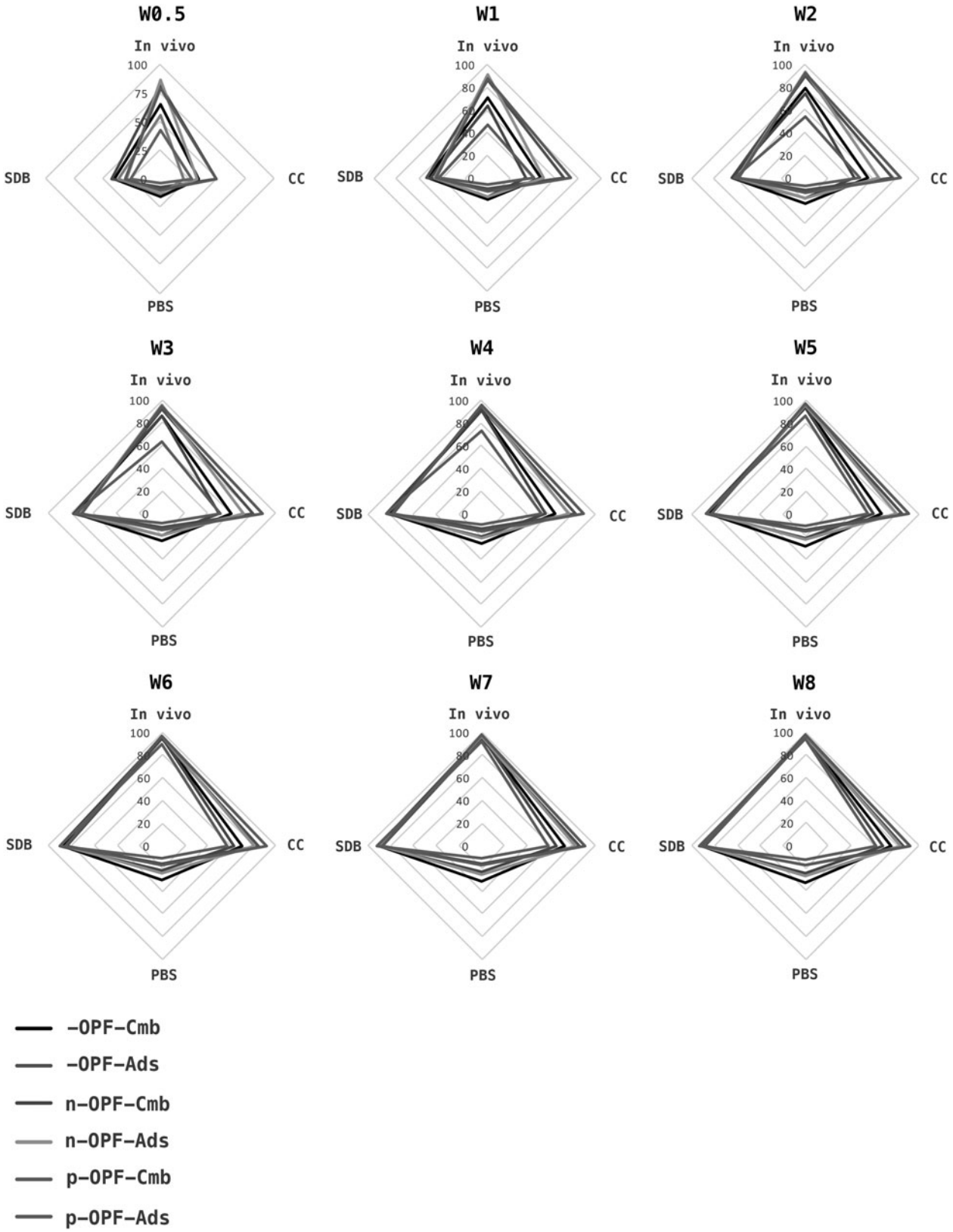

FIG. 6. Level D *in vitro* (CC, PBS, and SDB)-*in vivo* correlations (IVIVCs) of cumulative BMP-2 release (%) for a subset of OPF composites for all time points shown in radar diagrams per time point to analyze the rank order and extent of release of the different composites in the various release environments.

the tissue barriers (a nonlinear kinetic process), IVIVC models fail to accurately predict the *in vivo* drug performance under burst release conditions. Notably, in the cell culture *in vitro* environment, a strong linear model ($R^2 = 0.68$) with good internal predictability (residuals within ~10% BMP-2) was observed for the burst releases of the different composites. Since burst release is associated with a clinical relevant biological response and is often grossly underestimated *in vitro*,[14] predicting the *in vivo* burst release using an *in vitro* model could offer a highly valuable tool.

Composite modifications influenced the external predictability of the IVIVC. To achieve a robust level A IVIVC, external predictability of multiple composite formulations with different release rates are recommended.[12] The external predictability of the achieved IVIVCs is complicated by confounding effects of the different composite formulations. To address this issue, we studied a set of biomaterials with tunable BMP-2 loading method and surface chemistry resulting into differential BMP-2 release profile. Indeed, both the BMP-2 loading method and the composite surface chemistry influenced the relationship, slope, and intercepts of the IVIVC regression models. Therefore, the models were not superimposable and could not accurately predict the *in vivo* release profiles of other formulations. Other studies did achieve a level A IVIVC with multiple formulations.[29–32] However, these studies used relatively simple delivery vehicles of PLGA microspheres with varying molecular weight and/or lactic to glycolic ratio. These microspheres have comparable chemistry and release is directed by similar erosion and diffusion processes, while complex composites used in this study have different chemistry and release is directed by different mechanisms including polymer erosion, diffusion, desorption, and ion exchange. The differences between these release mechanisms *in vitro* and *in vivo* could have influenced the IVIVC of the different composites. Altogether these results indicate that for complex delivery vehicles, a more sophisticated *in vivo* prediction model is needed. Various confounding factors should be analyzed and implemented as variables for successful predictive modeling of *in vivo* BMP-2 release and bone formation. Therefore, standards need to be set within the field, including the preferable *in vitro* environment to study BMP-2 release.

There is an unmet need for tuned *in vitro* release environments for proper prediction of IVIVC. The IVIVCs of different composites were investigated in commonly used *in vitro* systems (PBS and cell culture setup) and an SDB. Thus far, these models have been employed and grossly underestimate the *in vivo* release and did not explore the IVIVC.[3,9,11,33,34] In all buffers of this study, IVIVCs with good internal predictive value could be developed, in line with other observations. However, in line with previous observations,[29,35,36] all models lacked external predictive value due to the confounding effect of the composite formulations. This implies that advanced systems are needed to accurately discriminate between various release profiles, predict burst release, and imitate the complex *in vivo* release mechanisms. Thus far, there are a few limited alternatives. Level A IVIVC based on multiple delivery vehicle formulations has been reported using membrane dialysis *in vitro* systems.[30,31] A flow through dissolution apparatus (USP 4), incorporating Risperdal microspheres or dexamethasone microspheres in laminar flow cells with PBS 0.1% (w/v) sodium azide as circulation medium, demonstrated improved discrimination between different release profiles, better prediction of the *in vivo* release profiles, and better prediction of the *in vivo* burst release.[32,37] These studies indicate that creating more *in vivo* reflective *in vitro* models could improve the predictive value of *in vitro* release kinetics.

Conclusion

The large differences between *in vitro* and *in vivo* release force us to reconsider the *in vitro* BMP-2 release models used in bone tissue engineering. The cell-free *in vitro* buffers (PBS and SDB) used in this study represented gross under- or overestimation of the *in vivo* release, respectively, and were not able to discriminate between different *in vivo* release profiles. Although the cell culture model performed better in discriminating the different *in vivo* release profiles the cumulative release was ranked differently compared with the *in vivo* ranking. All *in vitro* buffers showed IVIVCs with good internal predictive value. However, due to the confounding effect of composite formulations, all models lacked external predictability. To develop a predictive *in vitro* model for *in vivo* release from complex delivery vehicles, *in vitro* models should imitate the *in vivo* environment. Potential confounding effects of drug type, delivery vehicle formulations, and application site could be analyzed to develop one single IVIVC for release from complex delivery vehicles.

Acknowledgments

We thank James L. Herrick and Carl T. Gustafson of Mayo Clinic for technical support. The authors wish to acknowledge the National Institutes of Health (R01 AR45871 and R01 EB03060), AO Foundation (AO startup grant S-15-46K), Dutch Arthritis Foundation (LLP22), and Anna-NOREF foundation for their financial support.

Disclosure Statement

No competing financial interests exist.

References

1. Gothard, D., Smith, E.L., Kanczler, J.M., *et al.* Tissue engineered bone using select growth factors: a comprehensive review of animal studies and clinical translation studies in man. Eur Cells Mater **28,** 166; discussion 207, 2014.
2. Takita, H., Vehof, J.W., Jansen, J.A., *et al.* Carrier dependent cell differentiation of bone morphogenetic protein-2 induced osteogenesis and chondrogenesis during the early implantation stage in rats. J Biomed Mater Res A **71,** 181, 2004.
3. van de Watering, F.C., Molkenboer-Kuenen, J.D., Boerman, O.C., van den Beucken, J.J., and Jansen, J.A. Differential loading methods for BMP-2 within injectable calcium phosphate cement. J Control Release **164,** 283, 2012.
4. Yamamoto, M., Takahashi, Y., and Tabata, Y. Controlled release by biodegradable hydrogels enhances the ectopic bone formation of bone morphogenetic protein. Biomaterials **24,** 4375, 2003.
5. Kempen, D.H., Lu, L., Heijink, A., *et al.* Effect of local sequential VEGF and BMP-2 delivery on ectopic and orthotopic bone regeneration. Biomaterials **30,** 2816, 2009.

6. Li, B., Yoshii, T., Hafeman, A.E., Nyman, J.S., Wenke, J.C., and Guelcher, S.A. The effects of rhBMP-2 released from biodegradable polyurethane/microsphere composite scaffolds on new bone formation in rat femora. Biomaterials **30,** 6768, 2009.
7. Maire, M., Chaubet, F., Mary, P., Blanchat, C., Meunier, A., and Logeart-Avramoglou, D. Bovine BMP osteoinductive potential enhanced by functionalized dextran-derived hydrogels. Biomaterials **26,** 5085, 2005.
8. Brown, K.V., Li, B., Guda, T., Perrien, D.S., Guelcher, S.A., and Wenke, J.C. Improving bone formation in a rat femur segmental defect by controlling bone morphogenetic protein-2 release. Tissue Eng A **17,** 1735, 2011.
9. Kempen, D.H., Lu, L., Hefferan, T.E., *et al.* Retention of in vitro and in vivo BMP-2 bioactivities in sustained delivery vehicles for bone tissue engineering. Biomaterials **29,** 3245, 2008.
10. Rodriguez-Evora, M., Delgado, A., Reyes, R., *et al.* Osteogenic effect of local, long versus short term BMP-2 delivery from a novel SPU-PLGA-βTCP concentric system in a critical size defect in rats. Eur J Pharm **49,** 873, 2013.
11. Ruhe, P.Q., Boerman, O.C., Russel, F.G., Mikos, A.G., Spauwen, P.H., and Jansen, J.A. In vivo release of rhBMP-2 loaded porous calcium phosphate cement pretreated with albumin. J Mater Sci Mater Med **17,** 919, 2006.
12. FDA Guidance for Industry: Extended release oral dosage forms: Development, evaluation and application of in vitro/in vivo correlation. Available from: http://academy.gmp-compliance.org/guidemgr/files/1306FNL.PDF (accessed June 29, 2018).
13. Shen, J., and Burgess, D.J. In vitro-in vivo correlation for complex non-oral drug products: where do we stand? J Control Release **219,** 644, 2015.
14. Olthof, M.G., Kempen, D.H., Liu, X., *et al.* Bone morphogenetic protein-2 release profile modulates bone formation in phosphorylated hydrogel. J Tissue Eng Regen Med **12,** 1339, 2018.
15. Olthof, M.G., Kempen, D.H., Liu, X., *et al.* Phosphate functional groups improve oligo[(polyethylene glycol) fumarate] osteoconduction and BMP-2 osteoinductive efficacy. Tissue Eng Part A **24,** 819, 2018.
16. Poduslo, J.F., Curran, G.L., and Berg, C.T. Macromolecular permeability across the blood-nerve and blood-brain barriers. Proc Natl Acad Sci U S A **91,** 5705, 1994.
17. Kempen, D.H., Lu, L., Classic, K.L., *et al.* Non-invasive screening method for simultaneous evaluation of in vivo growth factor release profiles from multiple ectopic bone tissue engineering implants. J Control Release **130,** 15, 2008.
18. Shive, M.S., and Anderson, J.M. Biodegradation and biocompatibility of PLA and PLGA microspheres. Adv Drug Deliv Rev **28,** 5, 1997.
19. Dadsetan, M., Pumberger, M., Casper, M.E., *et al.* The effects of fixed electrical charge on chondrocyte behavior. Acta Biomater **7,** 2080, 2011.
20. Dadsetan, M., Szatkowski, J.P., Yaszemski, M.J., and Lu, L. Characterization of photo-cross-linked oligo[poly(ethylene glycol) fumarate] hydrogels for cartilage tissue engineering. Biomacromolecules **8,** 1702, 2007.
21. Hoaglin, D.C., Iglewicz, B., and Tukey, J.W. Performance of some resistant rules for outlier labeling. J Am Stat Assoc **81,** 991, 1986.
22. Lu, L., Peter, S.J., Lyman, M.D., *et al.* In vitro and in vivo degradation of porous poly(DL-lactic-co-glycolic acid) foams. Biomaterials **21,** 1837, 2000.
23. Xia, Z., and Triffitt, J.T. A review on macrophage responses to biomaterials. Biomed Mater **1,** R1, 2006.
24. Baxter, F.R., Bowen, C.R., Turner, I.G., and Dent, A.C. Electrically active bioceramics: a review of interfacial responses. Ann Biomed Eng **38,** 2079, 2010.
25. Lee, M., Chen, T.T., Iruela-Arispe, M.L., Wu, B.M., and Dunn, J.C. Modulation of protein delivery from modular polymer scaffolds. Biomaterials **28,** 1862, 2007.
26. Laffargue, P., Fialdes, P., Frayssinet, P., Rtaimate, M., Hildebrand, H.F., and Marchandise, X. Adsorption and release of insulin-like growth factor-I on porous tricalcium phosphate implant. J Biomed Mater Res **49,** 415, 2000.
27. Blanco-Príeto, M.J., Campanero, M.A., Besseghir, K., Heimgatner, F., and Gander, B. Importance of single or blended polymer types for controlled in vitro release and plasma levels of a somatostatin analogue entrapped in PLA/PLGA microspheres. J Control Release **96,** 437, 2004.
28. Jones, A.J., Putney, S., Johnson, O.L., and Cleland, J.L. Recombinant human growth hormone poly(lactic-co-glycolic acid) microsphere formulation development. Adv Drug Deliv Rev **28,** 71, 1997.
29. Chu, D.-F., Fu, X.-Q., Liu, W.-H., Liu, K., and Li, Y.-X. Pharmacokinetics and in vitro and in vivo correlation of huperzine A loaded poly(lactic-co-glycolic acid) microspheres in dogs. Int J Pharm **325,** 116, 2006.
30. D'Souza, S., Faraj, J.A., Giovagnoli, S., and DeLuca, P.P. IVIVC from long acting olanzapine microspheres. Int J Biomater **2014,** 407065, 2014.
31. D'Souza, S., Faraj, J.A., Giovagnoli, S., and DeLuca, P.P. In vitro-in vivo correlation from lactide-co-glycolide polymeric dosage forms. Prog Biomater **3,** 131, 2014.
32. Zolnik, B.S., and Burgess, D.J. Evaluation of in vivo-in vitro release of dexamethasone from PLGA microspheres. J Control Release **127,** 137, 2008.
33. Yamamoto, M., Ikada, Y., and Tabata, Y. Controlled release of growth factors based on biodegradation of gelatin hydrogel. J Biomater Sci Polym Ed **12,** 77, 2001.
34. Hernandez, A., Sanchez, E., Soriano, I., Reyes, R., Delgado, A., and Evora, C. Material-related effects of BMP-2 delivery systems on bone regeneration. Acta Biomater **8,** 781, 2012.
35. Li, X., Zhao, Z., Li, L., Zhou, T., and Lu, W. Pharmacokinetics, in vitro and in vivo correlation, and efficacy of exenatide microspheres in diabetic rats. Drug Deliv **22,** 86, 2015.
36. Schliecker, G., Schmidt, C., Fuchs, S., Ehinger, A., Sandow, J., and Kissel, T. In vitro and in vivo correlation of buserelin release from biodegradable implants using statistical moment analysis. J Control Release **94,** 25, 2004.
37. Rawat, A., Bhardwaj, U., and Burgess, D.J. Comparison of in vitro-in vivo release of Risperdal® Consta® microspheres. Int J Pharm **434,** 115, 2012.

Address correspondence to:
Lichun Lu, PhD
Department of Physiology and Biomedical Engineering
Mayo Clinic College of Medicine
200 First Street SW, MS 3-69
Rochester, MN 55905

E-mail: lu.lichun@mayo.edu

Received: January 21, 2018
Accepted: April 19, 2018
Online Publication Date: July 11, 2018